New Outlook on the Possible Existence
of Superheavy Elements in Nature*

A. Marinov[1)]**, S. Gelberg[1)], D. Kolb[2)], R. Brandt[3)], and A. Pape[4)]

[1)]*Racah Institute of Physics, Hebrew University, Jerusalem, Israel*
[2)]*Department of Physics, University GH Kassel, Germany*
[3)]*Kernchemie, Philipps University, Marburg, Germany*
[4)]*IReS−UMR7500, IN2P3−CNRS/ULP, Strasbourg, France*
Received November 19, 2002

Abstract—A consistent interpretation is given to some previously unexplained phenomena seen in nature in terms of the recently discovered long-lived high-spin super- and hyperdeformed isomeric states. The Po halos seen in mica are interpreted as being due to the existence of such isomeric states in corresponding Po or nearby nuclei that eventually decay by γ or β decay to the ground states of ^{210}Po, ^{214}Po, and ^{218}Po nuclei. The low-energy 4.5-MeV α-particle group observed in several minerals is interpreted as being due to a very enhanced α transition from the third minimum of the potential-energy surface in a superheavy nucleus with atomic number $Z = 108$ (Hs) and atomic mass number around 271 to the corresponding minimum in the daughter. © *2003 MAIK "Nauka/Interperiodica"*.

1. INTRODUCTION

The theoretical predictions in the 1960s [1−8] of the possible existence of very long-lived superheavy elements around $Z = 114$ and $N = 184$ stirred a lot of excitement among the nuclear scientific community and initiated the search for the possible existence of superheavy elements in nature. In the present paper, we concentrate on two independent well-established experimental results that are impossible to understand under the present common knowledge of nuclear physics. These puzzling data are, first, the observation, in mica minerals, of certain halos that have been attributed to the α decay of the short-lived ^{210}Po, ^{214}Po, and ^{218}Po nuclei [9−11] and, second, the observation in several minerals of a low-energy α-particle group with an energy of about 4.5 MeV [12−15].

Halos in mica, which consist of tiny concentric rings, have been known for a long time [16, 17]. For most of them, the measured radii of the rings fit within the known ranges of the various α-particle groups from ^{238}U or ^{232}Th decay chains. Therefore, they were correctly interpreted back in 1907 [16, 17] as being due to the existence of very small grains of ^{238}U or ^{232}Th in the centers of the corresponding halos,

which have been decaying, through their characteristic decay chains, since the time of crystallization of the crust of the Earth. However, other types of halos were discovered back in 1939 [9] and were thoroughly studied by Gentry [10]. These are the ^{210}Po, ^{214}Po, and ^{218}Po halos, which consist of, respectively, one, two, and three concentric rings, with radii equal to the ranges of the α-particle groups from the decay chains of the corresponding Po isotopes.[1)] These Po isotopes belong to the ^{238}U decay chain. However, their half-lives, as well as the half-lives of their β-decay parents, are short, and since rings belonging to their long-lived precursors are absent, their appearance in nature is puzzling [18].

Another puzzling phenomenon is the low-energy α-particle group, around 4.5 MeV, which has been seen in molybdenite [12], in thorite [13], in magnetite [14], and in OsIr [15]. The cleanest spectrum, where this group appears without observed residues from U isotopes decays, was obtained by Cherdyntsev *et al.* [14]. Based on chemical behavior (having volatile oxides) of the α emitter, it has been suggested that it might be due to a decay of an isotope of Eka−Os, the superheavy element with $Z = 108$ (Hs).[2)]

[1)]Colored pictures of various halos are given in [11].
[2)]Actually Cherdyntsev suggested naming element 108 sergenium, based on part of the great silk road in Kazakhstan (name Serika) where the studied mineral molybdenite was found (private communication from Yu. Lobanov).
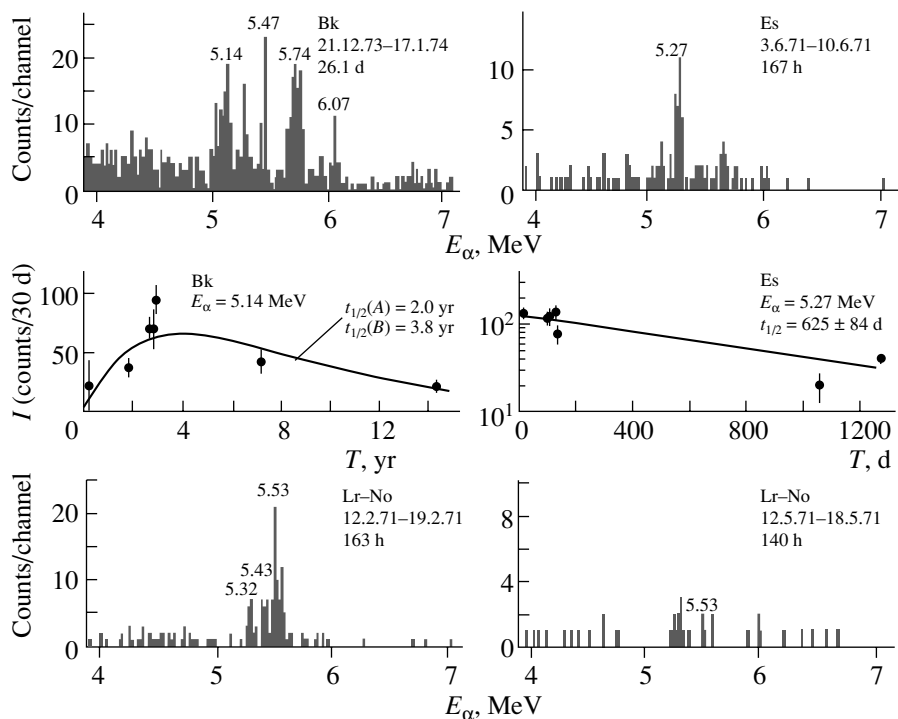
Fig. 1. Left, top: α-particle spectrum obtained with the Bk source. Right, top: α-particle spectrum obtained with the Es source. Left, center: decay curve obtained with the 5.14-MeV group seen with the Bk source (left, top above). {See Note (a) in Table 2 regarding the growing half-life of 2.0 yr [24].} Right, center: decay curve obtained with the 5.27-MeV group seen with the Es source (right, top above). Left, bottom: α-particle spectrum obtained with the Lr−No source. Right, bottom: the same as the previous one but taken about 3 months later. From a comparison of the two spectra a half-life of 26 ± 7 d was deduced for the 5.53-MeV group [24].

Since it was usually found together with ^{247}Cm and ^{239}Pu, it has been suggested [15] that this low-energy α-particle group is due to an isotope of element 108 which is a precursor of ^{247}Cm and its descendant ^{239}Pu. The half-life of this activity has been estimated to be around $(2.5 \pm 0.5) \times 10^8$ yr [12].

With the current common knowledge of nuclear physics, it seemed impossible to understand these data. The predicted energies of ground-state to ground-state α transitions for β stable Hs nuclei with atomic masses of 274 to 286 are between 9.5 and 6.7 MeV [19−21], and the predicted half-lives for these energies are between 3×10^{-2} s and 3×10^2 yr [22, 23], as compared to a half-life of about 5×10^{16} yr for 4.5 MeV. The question is why the nucleus decays with such a low-energy α-particle when a much higher energy, with a penetrability factor of at least 14 orders of magnitude higher, is available.

A second question is how the nucleus can decay with a lifetime that is about eight orders of magnitude shorter than what is predicted [22, 23] from energy versus lifetime relationships for a normal 4.5-MeV α-transition (experimentally estimated at 2.5×10^8 yr as

compared to the predicted value of 5×10^{16} yr). (A lifetime in the region of 10^{16} yr is certainly impossible, since it implies the existence of about 100 mg of material in the studied samples.)

In the following sections, similar effects seen in the study of various actinide fractions [24] produced via secondary reactions [25], and also in the study of the ^{16}O + ^{197}Au [26, 27] and the ^{28}Si + ^{181}Ta [28] heavy ion reactions, are summarized. Based on the results of all these experiments, a consistent interpretation for the puzzling phenomena seen in nature is suggested (see also [29]).

2. UNIDENTIFIED α-PARTICLE GROUPS IN ACTINIDES

In a study of actinide fractions from a W target that had been irradiated with 24-GeV protons, long-lived isomeric states were found in the neutron-deficient ^{236}Am and ^{236}Bk nuclei with respective half-lives of 0.6 yr and $\geq$30 d [30]. Their character, however, was not clear, being far from closed shell nuclei, where high-spin isomers are known, and living much longer than the known fission isomers. In addition, several unidentified α-particle groups were

Table 1. The energies and half-lives of several unidentified α-particle groups seen in various actinide sources as compared to theoretical predictions

Source	$E_\alpha^{\exp}$, MeV	$t_{1/2}^{\exp}$, yr	$t_{1/2}^{\text{cal}}$, yr [23]	Enhancement factor[c]	E_α (g.s. → g.s.), MeV[a]	$t_{1/2}^{\text{cal}}$, s[b]
Bk	5.14	3.8	1.7×10^5 [d]	4.5×10^4	6−7	2.2×10^9
Es	5.27	1.7	2.7×10^6 [e]	1.6×10^6	7−8	1.9×10^6
No−Lr	5.53	0.07	1.1×10^6 [f]	1.5×10^7	8−9	2.4×10^2

[a] Typical values from [33].

[b] Calculated for the lower energy of column 6 according to formulas given in [23].

[c] The ratio of column 4 to column 3.

[d] Calculated for ^{238}Am. See below.

[e] Calculated for ^{247}Es. See below.

[f] Calculated for ^{252}No. See below.

found in some actinide sources. Thus, 5.14-MeV ($t_{1/2} = 3.8 \pm 1$ yr), 5.27-MeV ($t_{1/2} = 625 \pm 84$ d), and 5.53-MeV ($t_{1/2} = 26 \pm 7$ d) groups were found, respectively, in the Bk, Es, and Lr−No sources [24, 30] (see Fig. 1 and Table 1). Similar to the situation with the 4.5-MeV group seen in nature, also here in the case of the latter unidentified groups, one cannot understand their relatively low energies [e.g., 5.53 MeV in Lr−No as compared to typical ground-state to ground-state transitions of around 8 MeV (column 6 of Table 1), which have penetrability factors about 11 orders of magnitude larger (the ratio of column 4 to column 7 in Table 1)] and their very enhanced character, having a factor of 10^5−10^7 shorter half-lives than predicted from the systematics of energy versus the half-life relationship for normal α decays [22, 23] (see column 5 in Table 1). The deduced evaporation-residue cross sections [24], in the mb region, are also several orders of magnitude larger than expected.

3. STUDY OF THE ^{16}O + ^{197}Au REACTION AND LONG-LIVED HIGH-SPIN SUPERDEFORMED ISOMERIC STATES

A possible explanation for the above puzzling data comes from the study of the ^{16}O + ^{197}Au reaction at $E_{\text{lab}} = 80$ MeV, which is around the Coulomb barrier [26, 27], and of the ^{28}Si + ^{181}Ta reaction at $E_{\text{lab}} = 125$ MeV [28], about 10% below the Coulomb barrier. In the first reaction, a 5.2-MeV α-particle group with a half-life of about 90 min has been found in ^{210}Fr. This group has the same unusual properties as the abnormal α-particle groups found in the actinides and produced via secondary reactions, and of the 4.5-MeV group found in nature. 5.2 MeV is a low energy as compared to 6.5 MeV, the ground-state to ground-state transition from ^{210}Fr, and the

90-min half-life is about 4×10^5 enhanced as compared to the prediction [22, 23] for normal α particles of this energy from ^{210}Fr. However, the 5.2-MeV group has been found in coincidence with γ rays which fit the energies of superdeformed band transitions. Therefore, the α decay is through a barrier of a superdeformed nucleus, and the large enhancement can quantitatively be understood [26] if one takes into account typical superdeformed radius parameters in the penetrability calculations. The data were consistently interpreted [26] in terms of production of a long-lived high-spin isomeric state in the second well of the potential energy surface of ^{210}Fr which decays, by a very enhanced α transition, to a high-spin state in the second well of ^{206}At.

The predicted [31, 32] excitation energies of the second minima in ^{210}Fr and nearby nuclei are above the proton separation energies [33]. Therefore, the decay of isomeric states from the second minima, by emitting protons, is in principle possible. In a separate study of the same ^{16}O + ^{197}Au reaction [27], long-lived proton radioactivities with half-lives of about 5.8 and 67.3 h have been discovered. They were interpreted as being due to very retarded decays from superdeformed isomeric states in the parent nuclei to normal deformed or to the ground states of the daughters. In particular, the indicated line with $E_p = 2.19$ MeV [27] may be associated with the predicted [31] ($E_p = 2.15$ MeV) second minimum to ground state transition from ^{198}Tl, which can be produced by three consecutive superdeformed to superdeformed α-transitions from ^{210}Fr.

4. STUDY OF THE ^{28}Si + ^{181}Ta REACTION AND LONG-LIVED HIGH-SPIN HYPERDEFORMED ISOMERIC STATES

The ^{28}Si + ^{181}Ta reaction has been studied at $E_{\text{lab}} = 125$ MeV, which is about 10% below the

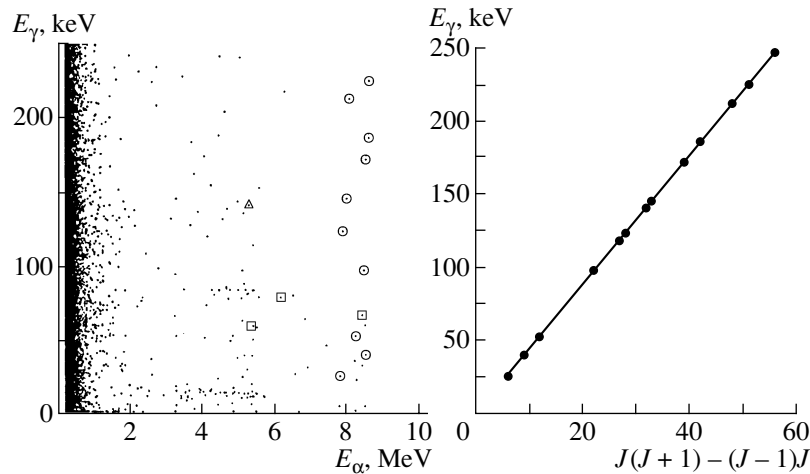**Fig. 2.** Left: α–γ coincidence plot from one measurement of the ^{28}Si + ^{181}Ta reaction. $E_{\text{lab}} = 125$ MeV, with 200-μg/cm^2 C catcher foil, taken for 76.8 d, starting 77.4 d after the end of irradiation. The γ-ray energies of the encircled events fit with SDB transitions. The squared events fit with known characteristic x rays and the events in triangles are identified with known γ-ray transitions (see [28]). Right: E_γ vs. $J(J+1) - (J-1)J$ for the γ rays seen in coincidence with 7.8–8.6 MeV α-particles. (The encircled events in the left figure plus similar events obtained in a second measurement [28].) The slope of the straight line is 4.42 keV.

Coulomb barrier, and at $E_{\text{lab}} = 135$ MeV [28]. A fusion cross section of about 10 mb is predicted at 125 MeV using a coupled-channel deformation code [34] with deformation parameters $\beta_2 = 0.41$ for ^{28}Si and $\beta_2 = 0.26$ for ^{181}Ta [35] and allowing for 2^+ and 3^- excitations in ^{28}Si. Only 2μb is predicted when no deformations are included in the calculations. For 135 MeV, the corresponding predicted fusion cross sections are 95 mb with deformations and 40 mb without.

Figure 2 (left) shows an α–γ two-dimensional coincidence plot obtained at $E_{\text{lab}} = 125$ MeV. Quite a few coincidence events are seen between a relatively

high energy α-particle group around 8.6 MeV and various γ rays. The half-life of this coincidence group has been measured [28] to be 40 d $\leq t_{1/2} \leq$ 2.1 yr. Figure 2 (right) shows that the γ rays which are in coincidence with these high-energy α particles fit nicely with a $J(J+1)$ law assuming $E_x = 4.42 \times J(J+1)$ keV and $\Delta J = 1$. On the basis of the observation of a Pt x ray in coincidence with the 8.6-MeV alphas and on kinematic arguments, it was suggested [28] that the α transition is from ^{195}Hg to ^{191}Pt. (^{195}Hg may be produced via $1p1n$ evaporation reaction and three consecutive III$^{\text{min}}$ → III$^{\text{min}}$ α decays, see below.) An energy parameter of 4.42 keV is typical to superdeformed band γ-ray transitions in this region of nuclei.

An α energy of 8.6 MeV is a very high energy for ^{195}Hg, which does not decay by emitting α particles, and its ground-state to ground-state Q_α value is 2.190 MeV [33]. A half-life of 40 d is about 13 orders of magnitude too long as compared to the systematics of energy vs. half-life relationship [23], which predicts $t_{1/2} \approx 6 \times 10^{-8}$ s. Since the α particles are in coincidence with superdeformed band γ-ray transitions, the α decay is to the superdeformed well of the daughter nucleus. However, it could not be a II$^{\text{min}}$ → II$^{\text{min}}$ transition, since such a transition is very enhanced as opposed to the large retardation measured in the experiment. A consistent interpretation, both from the point of view of the high energy of the α particles and their very long lifetime, is that the decay is from a long-lived high-spin ($J \approx 39/2$) isomeric state in the III$^{\text{min}}$, the hyperdeformed minimum [36–39] of
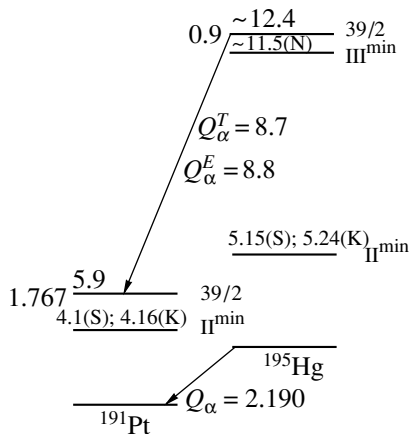

Fig. 3. Proposed decay scheme deduced from the observation of the 8.6-MeV α particles seen in coincidence with superdeformed band transitions. S—Satula *et al.* [31]; K—Krieger *et al.* [32]; N—Nazarewicz [37].

Table 2. A comparison between the experimental α-particle energies and values deduced from the predictions of [36] for some superdeformed (SD) to superdeformed and hyperdeformed (HD) to hyperdeformed isomeric transitions. (The last column shows the corresponding experimental ground-state to ground-state transitions [33].)

Source	E_α^{exp}, MeV	Isotope	Transition	E_α^{cal}, MeV [36]	$E_\alpha^{\mathrm{g.s}\to\mathrm{g.s}}$, MeV
Bk	5.14	^{238}Am[a]	SD $\to$ SD	5.13	5.94
Es	5.27	^{247}Es	HD $\to$ HD	5.27	7.32
No$-$Lr	5.53	^{252}No	HD $\to$ HD	≈ 5.6[b]	8.42

[a] Since the intensity of the 5.14-MeV group (Fig. 1) grew at the beginning with time, it was assumed here [24], similar to the situation with the isomeric states in ^{236}Bk and ^{236}Am [30], that ^{238}Bk decayed by EC or β^+ transitions to ^{238}Am.

[b] Extrapolated value. See [24].

Table 3. Experimental and predicted half-lives for superdeformed (SD) to superdeformed and hyperdeformed (HD) to hyperdeformed transitions [24]

Mother isotope	E_α, MeV	Transition	β_2[a]	β_3[a]	β_4[a]	$t_{1/2}^{\mathrm{cal}}$, yr[b]	$t_{1/2}^{\mathrm{exp}}$, yr
^{238}Am	5.14	SD $\to$ SD	0.71	0.0	0.09	10.9	3.8 ± 1.0
^{247}Es	5.27	HD $\to$ HD	1.05	0.19	0.0	1.15	1.7 ± 0.2
^{252}No	5.53	HD $\to$ HD	1.2	0.19	0.0	0.22	0.07 ± 0.02

[a] β_2 and β_4 values were deduced from the ϵ_2 and ϵ_4 values given in [36] using Fig. 2 of [40]. The value of β_3 was taken equal to ϵ_3.

[b] Calculated according to formulas given in [24]. Calculated half-lives for other deformation parameters are given in [24].

^{195}Hg, which decays by strongly retarded transition to the II$^{\mathrm{min}}$ of the potential in ^{191}Pt [28]. As seen in Fig. 3 the predicted Q_α value for such a transition is about 8.7 MeV, taking into account an extrapolated value from [37] for the excitation energy of the III$^{\mathrm{min}}$ in ^{195}Hg and the predictions of [31, 32] for the excitation energy of the II$^{\mathrm{min}}$ in ^{191}Pt. This value fits rather nicely with the measured Q_α value of about 8.8 MeV. (The excitation energy of the state in the third minimum of ^{195}Hg was assumed to be around the rotational 39/2 state with estimated energy of $E_x = 2.2 \times J(J+1)$ keV [39].)

5. SUPER- AND HYPERDEFORMED ISOMERIC STATES IN THE ACTINIDE REGION

Based on the discovery of the long-lived super- and hyperdeformed isomeric states (Sections 3 and 4), a consistent interpretation has been given [24] to the unidentified α-particle groups seen in the actinide sources and described in Section 2 above. II$^{\mathrm{min}} \to$ II$^{\mathrm{min}}$ and III$^{\mathrm{min}} \to$ III$^{\mathrm{min}}$ α-particle transition energies have been deduced from the predicted [36] excitation energies. Table 2 shows that the low-energy 5.14-, 5.27-, and 5.53-MeV groups, seen in the Bk, Es, and No$-$Lr sources can consistently be interpreted as being due to the low-energy II$^{\mathrm{min}} \to$ II$^{\mathrm{min}}$ transition from ^{238}Am and

III$^{\mathrm{min}} \to$ III$^{\mathrm{min}}$ transitions from ^{247}Es and ^{252}No, respectively. Their energies are considerably lower than the corresponding ground-state to ground-state transitions (column 6 in Table 2).

Table 3 shows that the very enhanced measured half-lives of the low-energy α-particle groups seen in the various actinide sources are consistent with
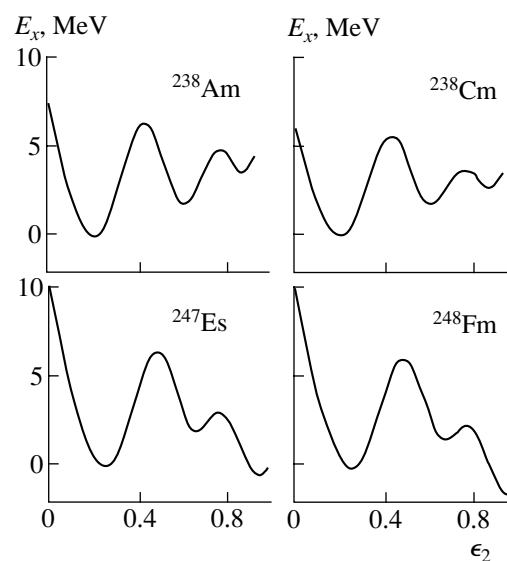

Fig. 4. Potential energies as function of quadrupole deformations for four nuclei according to [36].
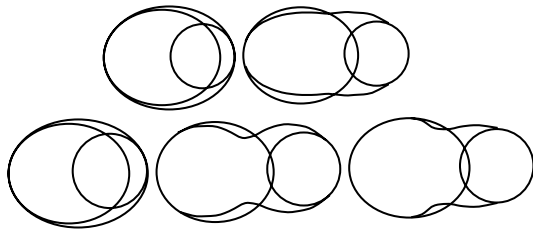
Fig. 5. Calculated shapes of two compound nuclei at various configurations together with the shapes of the corresponding projectile and target nuclei. Top, left: $A_{CN} = 239$ in the normal ground state; $\beta_2 = 0.2$; $\beta_4 = 0.08$ [36]. Top, right: $A_{CN} = 239$ in the second minimum; $\beta_2 = 0.77$; $\beta_4 = 0.1$ [36]. In both figures, $A_{heavy} = 186$; $\beta_2 = 0.22$ [35]. $A_{light} = 53$; $\beta_2, \beta_3, \beta_4 = 0$. Bottom, left: $A_{CN} = 253$ in the normal ground state; $\beta_2 = 0.28$; $\beta_4 = 0.01$ [36]. Bottom, center: $A_{CN} = 253$ in the third minimum; $\beta_2 = 1.2$; $\beta_4 = 0$ [36]. Bottom, right: $A_{CN} = 253$ with parameters of the third minimum of ^{232}Th; $\beta_2 = 0.85$; $\beta_3 = 0.35$; $\beta_4 = 0.18$ [38]. In the three figures at the bottom, $A_{heavy} = 186$; $\beta_2 = 0.22$ [35]. $A_{light} = 67$; $\beta_2, \beta_3, \beta_4 = 0$.

Fig. 6. Calculated fusion cross sections using the code CCDEF [34] for the ^{70}Zn + ^{186}W reaction assuming various quadrupole deformations of the projectile and target nuclei (see text, Section 5).

calculated values [24], taking into account in the penetrability calculations the deformation parameters of the superdeformed and hyperdeformed isomeric states.

The potential energies as function of quadrupole deformations, taken from [36], are shown in Fig. 4 for the ^{238}Am, ^{238}Cm, ^{247}Es, and ^{248}Fm nuclei. It is seen that, in ^{238}Am, the inner and the outer barriers of the second minimum are quite large, while in ^{247}Es and ^{248}Fm the outer barriers of the second minima are small, and the inner barriers of the third minima are large. In fact, the third minima in ^{247}Es and ^{248}Fm are predicted to be the ground states of these nuclei, being 0.61 and 1.76 MeV below the normal, slightly deformed, ground states. Unfortunately there are no predictions in these cases for the potential at even larger deformations, beyond the third minimum. (In the case of ^{232}Th [38], the outer barrier in the third minimum is quite high.)

In [24], detailed estimates for the various production cross sections of the actinide nuclei, as well as of the superheavy element with $Z = 112$ and $N \simeq 160$, are given. It is argued that the relatively large fusion cross sections, in the millibarn region, are due to two effects. First, the compound nucleus is produced in an isomeric state in the second or third minimum of the potential, rather than in the normal ground state. As shown in Fig. 5, much less overlapping and penetration are needed under these conditions, and therefore the compound nucleus formation probability increases drastically. Secondly, in the secondary reaction experiment, the projectile is a fragment that has been produced within 2×10^{-14} s befo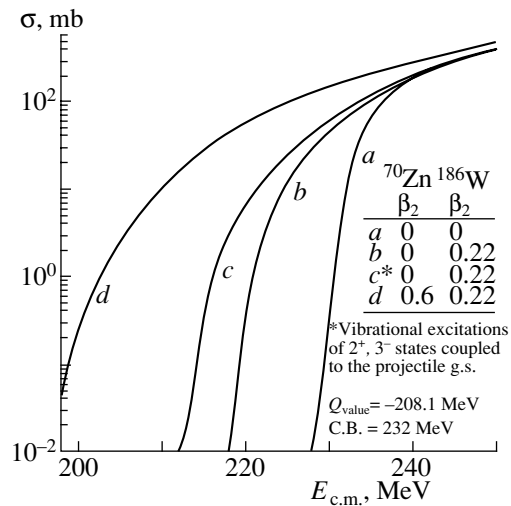re interacting with another W nucleus in the target. During this short time, it is at high excitation energy and quite deformed. Figure 6 gives the results of couple-channel calculations [34] for the fusion cross section as a function of bombarding energy for the ^{70}Zn + ^{186}W reaction, taking into account the known deformation of ^{186}W and various deformations of the projectile. In Fig. 6, curve d shows the results when the projectile has a deformation that is typical for the second minimum of the potential. It is seen that, due to the reduced Coulomb repulsion between the two nuclei for the tip to tip configuration, the cross section decreases very slowly with decreasing bombarding energy.

An idea about the relative importance of the above two effects can be deduced from the following arguments: the difference from a typical cross section of about 1 pb [41] obtained in the ^{70}Zn + ^{208}Pb reaction producing the nucleus ^{277}112 in its ground state to a cross section of about 20 nb producing $^{271(2)}$112 in an isomeric state via the ^{88}Sr + ^{184}W reaction [42] is due to the first effect. The additional difference from 20 nb to about 3.8 mb [24] of producing element 112 in an isomeric state via secondary reactions is due to the second effect.

6. SUMMARY OF THE PROPERTIES OF THE SUPER- AND HYPERDEFORMED ISOMERIC STATES

Figure 7 summarizes the results obtained about the super- and hyperdeformed isomeric states. The nucleus may have a long lifetime in its ground state, but also in long-lived isomeric states in the second
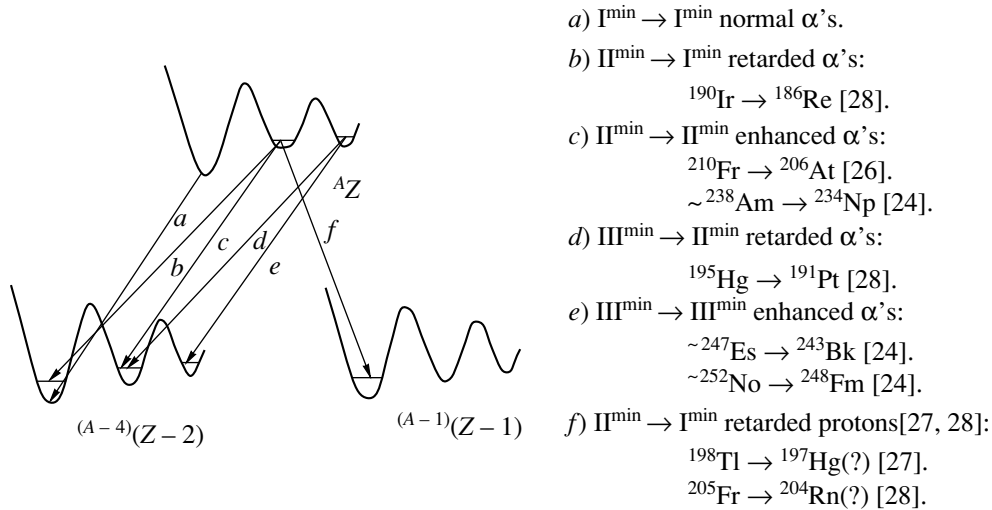
a) $I^{\min} \to I^{\min}$ normal α's.

b) $II^{\min} \to I^{\min}$ retarded α's:

^{190}Ir $\to$ ^{186}Re [28].

c) $II^{\min} \to II^{\min}$ enhanced α's:

^{210}Fr $\to$ ^{206}At [26].

$\sim^{238}$Am $\to$ ^{234}Np [24].

d) $III^{\min} \to II^{\min}$ retarded α's:

^{195}Hg $\to$ ^{191}Pt [28].

e) $III^{\min} \to III^{\min}$ enhanced α's:

$\sim^{247}$Es $\to$ ^{243}Bk [24].

$\sim^{252}$No $\to$ ^{248}Fm [24].

f) $II^{\min} \to I^{\min}$ retarded protons[27, 28]:

^{198}Tl $\to$ ^{197}Hg(?) [27].

^{205}Fr $\to$ ^{204}Rn(?) [28].

Fig. 7. Summary of abnormal particle decays seen in various experiments.

and third minima of the potential-energy surfaces. Long-lived superdeformed isomeric states may decay by very enhanced α particles to superdeformed states in the daughter nuclei or by strongly retarded α particles to the normal deformed states in the corresponding nuclei. It also may decay by very retarded proton radioactivity. Similarly, hyperdeformed isomeric states may decay by strongly enhanced α-particle decay to the hyperdeformed potential well in the daughter or by very retarded α decay to the superdeformed minimum in the same nucleus. All these extremely unusual decay properties have been discovered experimentally as summarized in Fig. 7.

It should be mentioned that the half-lives of the newly discovered isomeric states are longer than those of their corresponding ground states. Such a comparison for the isomeric states in the actinide region is presented in Table 4.

It should be mentioned that, back in 1969 [44], a new type of fission isomeric state was predicted for nuclei with $N \approx 144{-}150$. A specialization energy in excess of 4 MeV for the second barrier was predicted for a $[505]\frac{11}{2}^-$ state, which is associated with a factor of about 10^{15} increase in the half-life of a normal fission shape isomer.

7. SUPER- AND HYPERDEFORMED ISOMERIC STATES AND THE PUZZLING PHENOMENA SEEN IN NATURE

The discovered super- and hyperdeformed long-lived isomeric states enable one to understand the previously puzzling phenomena seen in nature (see the Introduction).

The source for the Po halos [9, 10] may be such isomeric states in isotopes with $Z \simeq 84$ that decayed, by β or γ decays, to the ground states of ^{210}Po, ^{214}Po, and ^{218}Po.

The low-energy α particles around 4.5 MeV [12–15] can consistently be interpreted as being due to a very enhanced $III^{\min} \to III^{\min}$ transition in $Z \sim 108$ and $A \sim 271$. The predicted [24, 26] half-life in this case is around 10^9 yr, as seen in Table 5. This resolves the first difficulty in understanding these data, namely, the lifetime about eight orders of magnitude shorter

Table 4. Half-lives of some isomeric states and their ratios to the half-lives of their corresponding normal-deformed ground states

Isotope	$t_{1/2}^{\text{g.s}}$	$t_{1/2}^{\text{i.s}}$	$t_{1/2}^{\text{i.s}}/t_{1/2}^{\text{g.s}}$
^{236}Bk	42.4 s[a]	$\geq$ 30 d[b]	$\geq 6.1 \times 10^4$
^{236}Am	3.6 min[c]	219 d[b]	8.8×10^4
^{238}Am[d]	98 min[e]	3.8 yr	2.0×10^4
^{247}Es[f]	4.55 min[e]	625 d	2.0×10^5
^{252}No[g]	2.3 s[e]	26 d	9.8×10^5

[a] Predicted by Möller *et al.* [19].

[b] Ref. [30].

[c] Nagame *et al.*, these Proceedings.

[d] Assuming that the 5.14-MeV group is from ^{238}Am (see Tables 1 and 3).

[e] Ref. [43].

[f] Assuming that the 5.27-MeV group is from ^{247}Es (see Tables 1 and 3).

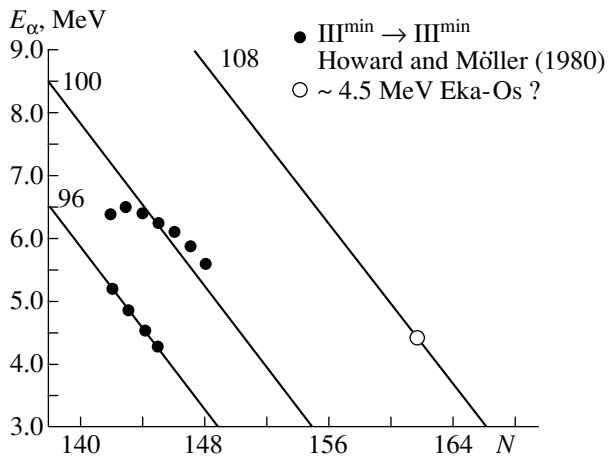[g] Assuming that the 5.53-MeV group is from ^{252}No (see text).

Fig. 8. Predictions [36], and extrapolations from these predictions, of the $III^{min} \to III^{min}$ α-particle energies. The black dots are the predictions for various isotopes of $Z = 96$ and $Z = 100$. The straight lines are extrapolations from these predictions. The open circle shows the position of 4.5-MeV α particles in $Z = 108$.

than what is predicted [22, 23] from the energy versus lifetime relationship for a normal α transition. (About 2.5×10^8 yr estimated experimentally as compared to 5×10^{16} yr. See the Introduction.)

In addition, an extrapolation of the deduced α energies for $III^{min} \to III^{min}$ transitions from the predictions of [36] shows that, for $Z = 108$, E_α of about 4.5 MeV corresponds to $N \sim 162$ (see Fig. 8). This is consistent with the suggestion [15] that ^{247}Cm may be a descendent of the superheavy element with $Z = 108$ which decays by 4.5-MeV α particles, since ^{247}Cm can be obtained from $^{271}_{108}$Hs$_{163}$ by six successive α decays. Another possibility is that the long-lived isotope is ^{267}Hs, which decays by two β^+ or electron capture decays to ^{267}Sg, which is then fol-

Table 5. Calculated half-lives for hyperdeformed to hyperdeformed α-particle transition of 4.5 MeV from ^{271}Hs assuming various deformation parameters [24]

β_2	β_3	β_4	$t_{1/2}$, yr
1.2[a]	0.0[b]	0.0[a]	1.8×10^{11}
1.2[a]	0.19[c]	0.0	4.6×10^9
0.85[d]	0.35[d]	0.18[d]	1.3×10^8

[a] ϵ_2 and ϵ_4 values for ^{248}Fm were taken from [36] and converted to β_2 and β_4 values according to [40].

[b] Assuming $\beta_3 = 0$.

[c] Assuming $\beta_3 = \epsilon_3$ of [36].

[d] Parameters given in [38] for ^{232}Th.

lowed by five successive α decays to ^{247}Cm. It should, however, be mentioned that, in principle, the above 4.5-MeV α particles may also be due to a strongly retarded $II^{min} \to I^{min}$ or $III^{min} \to II^{min}$ transition in the region of Os itself. (For normal 4.5-MeV α particles in Os, the expected [22, 23] half-life is about 1 yr. Such a short-lived nuclide cannot exist in nature.)

8. SUMMARY

It was shown that the newly discovered long-lived super- and hyperdeformed isomeric states can provide consistent interpretations to two previously unexplained phenomena seen in nature. Thus, the Po halos can be understood as being due to the existence of such isomeric states in nuclei with Z values around 84 and atomic masses in the region of 210−218. The observed 4.5-MeV α-particle group can be understood as being due to a low-energy and strongly enhanced hyperdeformed to hyperdeformed transition in a nucleus with $Z = 108$ and $A \simeq 271$.

It seems to us that the existence of superheavy elements in nature is not impossible.

ACKNOWLEDGMENTS

REFERENCES

1. V. M. Strutinsky, Yad. Fiz. **3**, 614 (1964) [Sov. J. Nucl. Phys. **3**, 449 (1964)].
2. W. D. Myers and W. J. Swiatecki, Nucl. Phys. **81**, 1 (1966).
3. A. Sobiczewski, F. A. Gareev, and B. N. Kalinkin, Phys. Lett. **22**, 590 (1966).
4. V. M. Strutinsky, Nucl. Phys. A **95**, 420 (1967).
5. C. L. Wong, Phys. Rev. Lett. **19**, 328 (1967).
6. Yu. A. Muzychka, V. V. Pashkevich, and V. M. Strutinsky, Preprint No. R7-3733, JINR (Joint Inst. for Nucl. Res., Dubna, 1968).
7. S. G. Nilsson, J. R. Nix, A. Sobiczewski, *et al.*, Nucl. Phys. A **115**, 545 (1968).
8. J. Grumann, U. Mosel, B. Fink, and W. Greiner, Z. Phys. **228**, 371 (1969).
9. G. H. Henderson and F. W. Sparks, Proc. R. Soc. London, Ser. A **173**, 238 (1939).
10. R. V. Gentry, Science **160**, 1228 (1968).
11. R. V. Gentry, *Creation's Tiny Mystery* (Earth Sci. Associates, Knoxville, Tennessee, 1992).
12. V. V. Cherdyntsev and V. F. Mikhailov, Geochemistry, No. 1, 1 (1963).
13. R. D. Chery, K. A. Richardson, and J. A. S. Adams, Nature **202**, 639 (1964).
14. V. V. Cherdyntsev, V. L. Zverev, V. M. Kuptsov, and G. I. Kislitsina, Geochemistry, No. 4, 355 (1968).
15. H. Meier, W. Albrecht, D. Börche, *et al.*, Z. Naturforsch. **25**, 79 (1970).

16. J. Joly, J. Phil. Mag. **13**, 381 (1907).
17. O. Mugge, Zent. Mineral. **1907**, 397 (1907).
18. N. Feather, Cumm. Roy. Soc. Edinburgh, No. 11, 147 (1978).
19. P. Möller, J. R. Nix, and K.-L. Kratz, At. Data Nucl. Data Tables **66**, 131 (1997).
20. H. Koura, M. Uno, T. Tachibana, and M. Yamada, Nucl. Phys. A **674**, 47 (2000); RIKEN-AF-NP-394 (2001).
21. S. Liran, A. Marinov, and N. Zeldes, Phys. Rev. C **62**, 047301 (2000); nucl-th/0102055.
22. V. E. Viola, Jr. and G. T. Seaborg, J. Inorg. Nucl. Chem. **28**, 741 (1966).
23. G. Royer, J. Phys. G **26**, 1149 (2000).
24. A. Marinov, S. Gelberg, D. Kolb, and J. L. Weil, Int. J. Mod. Phys. E **10**, 209 (2001).
25. A. Marinov, C. J. Batty, A. I. Kilvington, *et al.*, Nature **229**, 464 (1971).
26. A. Marinov, S. Gelberg, and D. Kolb, Mod. Phys. Lett. A **11**, 861 (1996).
27. A. Marinov, S. Gelberg, and D. Kolb, Mod. Phys. Lett. A **11**, 949 (1996).
28. A. Marinov, S. Gelberg, and D. Kolb, Int. J. Mod. Phys. E **10**, 185 (2001).
29. A. Marinov, S. Gelberg, D. Kolb, *et al.*, in *Proceedings of the 3rd International Conference on Exotic Nuclei and Atomic Masses, Hämeenlinna, Finland, 2001*, Ed. by J. Äysto *et al.*, p. 380.
30. A. Marinov, S. Eshhar, and D. Kolb, Phys. Lett. B **191**, 36 (1987).
31. W. Satula, S. Ćwiok, W. Nazarewicz, *et al.*, Nucl. Phys. A **529**, 289 (1991).
32. S. J. Krieger, P. Bonche, M. S. Weiss, *et al.*, Nucl. Phys. A **542**, 43 (1992).
33. G. Audi and A. H. Wapstra, Nucl. Phys. A **565**, 66 (1993).
34. J. Fernández-Neillo, C. H. Dasso, and S. Landowne, Comput. Phys. Commun. **54**, 409 (1985).
35. S. Raman, C. H. Malarkey, W. T. Milner, *et al.*, At. Data Nucl. Data Tables **36**, 1 (1987).
36. W. M. Howard and P. Möller, At. Data Nucl. Data Tables **25**, 219 (1980).
37. W. Nazarewicz, Phys. Lett. B **305**, 195 (1993).
38. S. Ćwiok, W. Nazarewicz, J. X. Saladin, *et al.*, Phys. Lett. B **322**, 304 (1994).
39. A. Krasznahorkay, M. Hunyadi, M. N. Haraken, *et al.*, Phys. Rev. Lett. **80**, 2073 (1998).
40. W. Nazarewicz and I. Ragnarsson, *Handbook of Nuclear Properties*, Eds. by D. N. Poenaru and W. Greiner (Clarendon Press, Oxford, 1996), p. 80.
41. S. Hofmann, V. Ninov, F. P. Hessberger, *et al.*, Z. Phys. A **354**, 229 (1996).
42. A. Marinov, S. Gelberg, and D. Kolb, in *Conference "Nuclei Far from Stability/Atomic Masses and Fundamental Constants," 1992*, p. 437.
43. R. B. Firestone, V. S. Shirley, C. M. Baglin, *et al.*, *Table of Isotopes* (Wiley-Interscience, 1996).
44. S. G. Nilsson, G. Ohlén, C. Gustafsson, and P. Möller, Phys. Lett. B **30B**, 437 (1969).